

Dynamics of domain walls in an incommensurate phase near the lock-in transition: One-dimensional crystal model

S. V. Dmitriev* and T. Shigenari

Department of Applied Physics and Chemistry, University of Electro-Communications, Chofu-shi, Tokyo 182, Japan

A. A. Vasiliev

Department of Mathematical Modeling, Tver State University, 33, Zhelyabov st., 170000, Tver, Russia

K. Abe

Department of Applied Physics and Chemistry, University of Electro-Communications, Chofu-shi, Tokyo 182, Japan

(Received 25 October 1996)

A phase transition from a high-symmetry to a low-symmetry commensurate phase through an incommensurate phase was studied in the framework of the one-dimensional elastically hinged molecule model which includes only a fourth-order anharmonic potential. The phase diagram with respect to the harmonic-potential coefficient and the external force was obtained. From the numerical analysis of the equation of motion, it was shown that the incommensurate phase near the lock-in transition contains a periodic system of energetically equivalent domain walls which are mutually repulsive. The properties of the domain walls were studied and the lock-in transition was described as the annihilation process of the walls when the repulsion is changed to attraction. [S0163-1829(97)01614-7]

I. INTRODUCTION

The incommensurate (IC) phase of various crystals exists in a temperature range between high-symmetry and low-symmetry commensurate phases.^{1,2} The lower-temperature transition from the IC phase to a low-symmetry phase at T_c is a first-order transition, and the higher-temperature transition from a high-symmetry to an IC phase at T_i is a continuous structural transition of second order. The condensation of a soft mode in a certain point inside the Brillouin zone at T_i generates the IC phase as a modulated structure. Near T_i the modulation has the sinusoidal form but further cooling towards T_c changes the modulation to a rectangular form which can be considered as an array of commensurate domains separated by the discommensurations (domain walls). As a result of the so-called lock-in transition at T_c , the walls disappear and the commensurate structure with an elementary period, which is usually a multiple of the basic period of the high-symmetry phase, is formed. The existence of a periodic array of domains within the IC phase was observed in Rb_2ZnCl_4 by transmission electron microscopy.³ The six types of domains which differ either by the direction of their spontaneous polarization or by the relative translational phase shifts were observed (see the comments on Ref. 3 in Ref. 2). The process of nucleation and annihilation of discommensurations in the first-order IC-commensurate transition in K_2ZnCl_4 have been studied by Sakata *et al.*⁴ and Hamano *et al.*⁵ using etching, powder, replica, and transmission-electron microscopy techniques.

The first theoretical investigations of IC phases were provided within the framework of the phenomenological Landau theory.^{1,2,6} In contrast, the microscopic theories of displacive modulation take into account the discrete structure of the system and usually use an empirical description of interatomic interactions.¹ The model proposed here belongs to the

second type. The finding of the sufficient conditions for IC phase formation is one of the central applications of such models. For the IC phase formation in the frame of the Frenkel-Kontorova model, the period of a sinusoidal background potential and equilibrium interatomic distance of harmonically coupled chain must be different (see the contribution of Pokrovsky *et al.* in Ref. 7). For the models with a double-well background potential, not only the first- but also the second-neighbor harmonic interatomic interaction should be taken into account.⁸ In order to obtain the model with the acoustic mode, Janssen and Tjon⁹ did not introduce any background potential but in this case they showed that the presence of the third-neighbor interaction is essential for the IC phase formation and at least one of the coefficients should be negative to produce the competing interactions. The model of Chen and Walker¹⁰ with the competing interactions has a reach phase diagram which they studied to explain the sequences of phase transitions in various crystals of the A_2BX_4 family.

All the above models are one dimensional and each atom has one degree of freedom. Two-dimensional models were also studied by Parlinski and two-dimensional IC modulations ($2q$) were observed.¹¹

The microscopic models usually deal with a phase transition from a high-symmetry to an IC phase. We do not know an adequate description of the lock-in transitions. In this paper, we propose an elastically hinged molecule (EHM) model of a crystal. In the frame of the model, the lock-in transition can be treated as a result of motion and annihilation of domain walls. Janssen,¹ discussing the lock-in transition, pointed out that the discommensurations arrange themselves in the ground state in such a way that they are equidistant as possible. The conditions when this situation does not take place will be found in the present model. The annihilation (fusion) of domain walls colliding with the

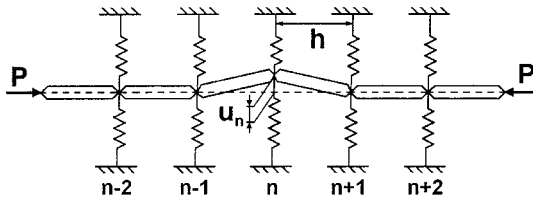


FIG. 1. The chain of molecules of length h connected by the hinges (EHM model). The action of the background potential is depicted by springs; u_n denotes the displacement of n th hinge. The chain is compressed by the force p along its axis.

small velocity was found for the φ^4 equation by Aubry.¹² Besides this process, another channel of the annihilation of domain walls was found for the EHM model. The nucleation and evolution of the discommensurations in two- and three-dimensional crystalline models have been studied also in Refs. 13 and 14.

The EHM model consists not of atoms but of molecules connected by hinges. The Hamiltonian of the model is identical to that for a linear chain with a local fourth-order polynomial potential and harmonic first- and second-neighbor interactions. The last model has already been studied⁸ but only for the double-well background potential and usually it treats only the case of a modulation with a long-wavelength soft mode. Here the case of a single-well fourth-order potential and the transitions with short-wavelength soft modes will be considered. One will see that for the formation of IC structure, the background potential does not need to be double well. In the frame of the EHM model for the IC phase formation the presence of the pressure term is necessary. The influence of the external compression on the commensurate-incommensurate phase transition has been studied numerically by Parlinski *et al.*¹⁵ It has also been studied experimentally. The temperature region of the IC phase in quartz (SiO_2) becomes wider with the increase of the external uniaxial stress and the $1q$ state increases proportional to the magnitude of stress.^{16,17} The width of the IC phase increases with hydrostatic pressure in NaNO_2 .^{18,19} Physically, taking into account the pressure term does not necessarily mean the presence of the external pressure. In some cases, e.g., in quartz, one may consider a two- or three-dimensional crystal as a set of chains of molecules a subset of which may be in compression but other chains in tension so that the averaged deformation of the crystal is equal to zero.

In Sec. II we describe the EHM model of a crystal and in Sec. III the phase diagram of the model is plotted. Section IV is concerned with the description of the change of the regime from a sinusoidal modulation to an array of domain walls. Finally in Sec. V, the static and dynamic properties of the domain walls and the possible lock-in transition are discussed. The partial results of Secs. II and III were reported in Ref. 20.

II. EHM MODEL OF CRYSTAL

Let us consider that the one-dimensional model of a crystal consists of the undeformable molecules of length h which are connected with each other by the elastic hinges (see Fig. 1). The hinges of the chain and the molecules are numbered

by integer-valued index n so that the n th molecule has hinges with numbers n and $n+1$. Each hinge has one degree of freedom, namely, the transversal displacement u_n . If the angle between the axes of the neighboring molecules is not equal to 0, the elastic hinge produces the moment which tends to decrease the absolute value of the angle. The stiffness of the hinge is characterized by the coefficient f . The hinges are in the anharmonic background potential $(r/2)u_n^2 + (s/4)u_n^4$. Finally, suppose that the chain of molecules is compressed by the force $p \geq 0$ along its axis.

In this paper we will consider the limiting case of small displacements ($u_n \ll h$). Under this assumption the angle of rotation of the n th molecule α_n can be expressed in terms of displacements as

$$\alpha_n = \frac{\Delta u_n}{h}, \quad (2.1)$$

where $\Delta u_n = u_{n+1} - u_n$.

The potential energy of the crystal can be written as

$$U = \frac{f}{2} \sum_n (\alpha_n - \alpha_{n-1})^2 + \sum_n \left(\frac{r}{2} u_n^2 + \frac{s}{4} u_n^4 \right) - \frac{P}{2h} \sum_n \Delta u_n^2. \quad (2.2)$$

The first term on the right-hand side of Eq. (2.2) is the potential energy accumulated by the hinges, the second term is the energy of hinges in the background potential, and the third term represents the work of the compression force. The expression $\frac{1}{2h} \Delta u_n^2$ in the last term represents the change of the horizontal projection of the molecule due to its rotation.

The mass of the molecule m is concentrated in its hinges. The Hamiltonian of the one-dimensional crystal $H_0 = U + (m/2) \sum (du_n/dt)^2$ may be written in the following form:

$$H = \frac{1}{2} \sum_n \left[\left(\frac{dy_n}{d\tau} \right)^2 + F(\Delta y_n - \Delta y_{n-1})^2 \right] + \frac{1}{2} \sum_n \left[-P\Delta y_n^2 + R y_n^2 + \frac{S}{2} y_n^4 \right], \quad (2.3)$$

where $y_n = u_n \sqrt{|s|/|r|}$, $\tau = t \sqrt{|r|/m}$, $H = H_0 |s|/r^2$, $F = f/(|r|h^2)$, $P = p/(|r|h)$, $R = r/|r| = \pm 1$, $S = s/|s| = \pm 1$.

It can be shown that this is the Hamiltonian for a linear chain with a local potential of the form of a fourth-order polynomial and harmonic first- and second-neighbor interactions. If $R = -1$ and $S = 1$, the local potential is a double-well potential, but below we consider the case $R = S = 1$ in which the potential has a single minimum.

From the Hamiltonian (2.3) the following equation for motion of the n th hinge may be obtained:

$$\frac{d^2 y_n}{d\tau^2} + F(y_{n-2} - 4y_{n-1} + 6y_n - 4y_{n+1} + y_{n+2}) + P(y_{n-1} - 2y_n + y_{n+1}) + y_n + y_n^3 = 0. \quad (2.4)$$

A few types of periodic solutions to Eq. (2.4), for which $y_n = y_{n+N}$, can be easily found. Obviously, it has a trivial solution

$$y_n = 0, \quad n = 0, \pm 1, \pm 2, \dots \quad (2.5)$$

The solution with the period $N=2$,

$$y_{2n} = -y_{2n-1} = Y_2, \tag{2.6}$$

where $Y_2^2 = 4P - 16F - 1$, which is possible if $P > 4F + 1/4$.

The solution with the period $N=3$,

$$y_{3n} = Y_3, \quad y_{3n-1} = y_{3n-2} = kY_3, \tag{2.7}$$

where $Y_3^2 = -(2k+1)/(2k^3+1)$, $3k = a - \sqrt[3]{2bg^{-1/3}} + (1/\sqrt[3]{2})g^{1/3}$, $a = 1/(6F-2P)$, $b = -a(a+3)$, $d = 2a^3 + 9a^2 - 27/2$, $g = d + \sqrt{4b^3 + d^2}$. This solution exists if $P > 3F + 1/3$ and $-1/\sqrt[3]{2} < k \leq -1/2$.

The four-periodic solution

$$y_{4n} = y_{4n-1} = -y_{4n-2} = -y_{4n-3} = Y_4, \tag{2.8}$$

where $Y_4^2 = 2P - 4F - 1$, exists if $P > 2F + 1/2$.

Substituting solutions (2.5)–(2.8) into the Hamiltonian (2.3), one finds the following expressions for the potential energy per molecule:

$$U_1 = 0, \tag{2.9}$$

$$U_2 = -\frac{1}{4} (-4P + 16F + 1)^2, \tag{2.10}$$

$$U_3 = \frac{1}{3} \left((3F - P)(1 - k)^2 + k^2 + \frac{1}{2} \right) Y_3^2 + \frac{1}{12} (2k^4 + 1) Y_3^4, \tag{2.11}$$

$$U_4 = -\frac{1}{4} (-2P + 4F + 1)^2 \tag{2.12}$$

for the trivial solution and for two-, three-, and four-periodic solutions, respectively.

III. PHASE DIAGRAM

In the subsequent discussion the parameters P and F will be considered temperature dependent. Changing of the temperature leads to the changing of the parameters, which can be described as the motion of the representative point in the phase space.

In Fig. 2 the phase diagram of the model is plotted in the P, F plane. The parabola 1 ($F = P^2/4$) and the straight line 2 ($F = P/4 - 1/16$) smoothly join at the point $[P(2), F(2)]$ and they define the boundary of the region where only the trivial solution exists.

Let the representative point move very slowly in the phase space from the region where the trivial solution is stable and crosses the boundary of stability. From the linearized equation (2.4) it follows that when the point crosses the boundary a new pattern appears gradually. It can be regarded as the freezing of the soft mode since the appearance of a new stationary solution means a change in the symmetry of the system and therefore a phase transition. The soft mode is proportional to the function

$$y_n = \sin(2\pi n \kappa), \tag{3.1}$$

where

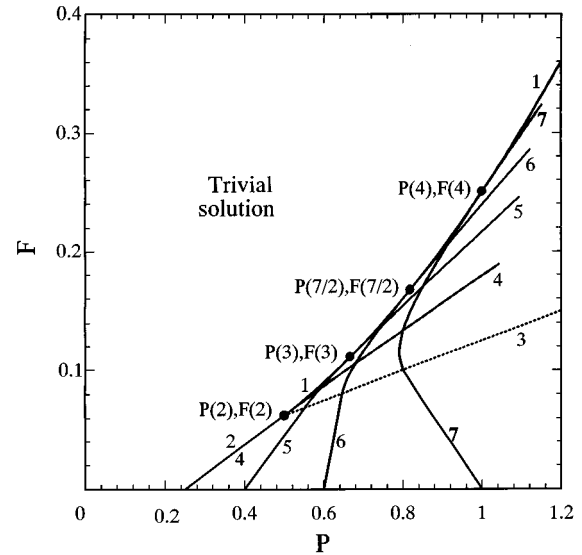


FIG. 2. The phase diagram of the model in the P, F plane. Curve 1 is the parabola $F = P^2/4$ and line 2 is $F = P/4 - 1/16$. Curves 4–7 are the hyperbolas (3.8) for $\lambda = 2, 3, 7/2, 4$, respectively. The points of tangency of hyperbolas 4–7 with parabola 1 are marked by the solid circles. The dashed line 3 is $F = P/8$.

$$\kappa = \frac{1}{\pi} \arcsin \sqrt{P/(8F)} \quad \text{for } F > \frac{P}{8} \tag{3.2}$$

and

$$\kappa = \frac{1}{2} \quad \text{for } F \leq \frac{P}{8}. \tag{3.3}$$

In the first case the point crosses the parabola 1 and the wavelength of the soft mode $\lambda = 1/\kappa$ is the function of the P, F . In the second case the point crosses line 2 and the structure (2.6) with period 2 is formed. In fact, the crystal structure necessarily will contain the randomly spaced domain walls forming due to the random nucleation process.

Let us discuss the stability of the modes with the rational wavelength

$$\lambda = \frac{N}{M}, \quad M = 1, 2, \dots, \quad N \geq 2M, \tag{3.4}$$

where N, M are given coprime numbers. Such a mode has a period N and it changes the sign $2M$ times within a period. The mode with wavelength $\lambda > 2$ appears when the representative point crosses parabola 1 at the point with the coordinates

$$P(\lambda) = \frac{1}{2} \left(\sin \frac{\pi}{\lambda} \right)^{-2}, \quad F(\lambda) = \frac{P^2(\lambda)}{4}. \tag{3.5}$$

The solution of the nonlinear equation of motion (2.4) along a path of the representative point was found numerically. The periodic boundary conditions and the trivial initial conditions with very small perturbation were assumed. In the immediate vicinity of the parabola 1 or the line 2 the displacements are small. In this region the influence of the nonlinear term is small and one can expect that the nonlinear Eq. (2.4) retains the principal properties of the associated linear-

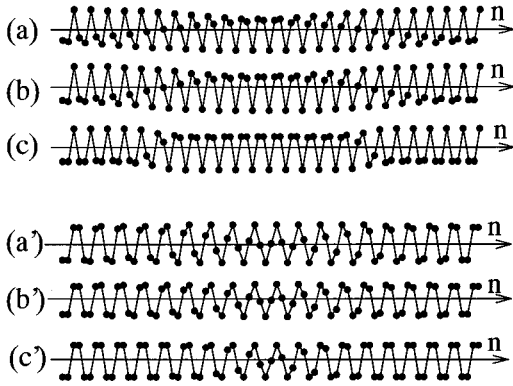


FIG. 3. The evolution of the crystal structure along the line $F=F(\lambda)$, (a)–(c) for $\lambda=76/25$ and (a')–(c') for $\lambda=77/19$. In (a), (a'), the structures in the immediate vicinity of parabola 1 are presented. In (b), (b') and (c), (c'), the structures for increasing magnitudes of P are shown. In (c) the low-symmetry three-periodic structure with two domain walls per 76 molecules is formed. In (c') there is the low-symmetry four-periodic structure with one domain wall per 77 molecules. The amplitude of displacements increases with P , but for these pictures they were normalized to the same value.

ized equation. Computer calculations show that it is so. It was found that after the representative point crosses the parabola at the point $[P(\lambda), F(\lambda)]$, the N -periodic solution which changes the sign $2M$ times within one period was formed. The same number of signs changes has the soft mode (3.1) obtained from the linearized equation of motion. If M is big enough the N -periodic solution ($N > 2M$) may be considered as the IC phase. In other words, crossing parabola 1 by the representative point at the point $[P(\lambda), F(\lambda)]$, where λ has a big denominator, is the phase transition from the high-symmetry phase (trivial solution) to the IC phase.

Numerical calculations show that when the representative point moves away from the parabola, the number of sign changes of the solution does not change. However, the transformation of the IC structure takes place and it reduces to the formation of a new low-symmetry N^* -periodic phase with wavelength $\lambda^*=N^*/M^*$ which is close to $\lambda=N/M$ but with a significantly smaller period $N^* \ll N$. As a result of the process, a set of domain walls appears. The density of domain walls can be expressed as

$$\rho = \frac{K}{N} |NM^* - MN^*|, \quad (3.6)$$

where $K=1$ or 2 for an even or an odd N^* , respectively. If N^* is an even number the N^* -periodic structure has only one type of domain, but if N^* is an odd number, there are $+$ and $-$ domains.

In the following, we shall find for a given path the point in the phase diagram from which the discommensurations exist in the form of domain walls by the comparison of the energies of the IC and the low-symmetry phases.

In Figs. 3(a)–3(c), the structure transformation described above is presented for the path of the representative point $F=F(76/25)$. Note, that $\lambda=76/25$ is only slightly greater than 3. In Fig. 3(a) the structure in the immediate vicinity of parabola 1 is shown. It is the 76-periodic solution with 50

sign changes within a period. In Figs. 3(b) and 3(c), the structures for increasing magnitudes of P are shown. In Fig. 3(c), the low-symmetry three-periodic structure with two domain walls per 76 molecules is formed. There are domains of two types.

In Figs. 3(a')–3(c') the same results but for path $F=F(77/19)$ are presented. Now $\lambda=77/19$ is close to 4. In the immediate vicinity of parabola 1, the 77-periodic solution with 38 sign changes within a period is formed. In Fig. 3(c') the low-symmetry four-periodic structure with one domain wall per 77 molecules is formed. There is only one type of domain.

We shall use the following results related to the phase diagram (Fig. 2). The equilibrium solution which appears after the representative point crosses parabola 1 at the point $[P(\lambda), F(\lambda)]$, $\lambda \geq 2$ exists in the area where

$$F > \frac{P(\lambda)}{2} P - F(\lambda). \quad (3.7)$$

The boundary of the stability region for this solution is the hyperbola

$$F^2 + \frac{F(\lambda)}{12} P^2 - \frac{P(\lambda)}{2} FP + \frac{2F(\lambda)}{3} F < 0 \quad (3.8)$$

in the region $F > P/8$ and the smoothly joined straight line

$$F > \frac{P-Q}{G} + \frac{Q}{8} \quad (3.9)$$

in the region $F \leq P/8$, where $G = [32F(\lambda) - 6]/[8F(\lambda) - 3P(\lambda)]$, $Q = [16F(\lambda)]/[12P(\lambda) - 16F(\lambda) - 3]$. The joining takes place at the line $F = P/8$. The hyperbola (3.8) is tangent to parabola 1 at the point $[P(\lambda), F(\lambda)]$. Curves 4–7 in Fig. 2 are the boundaries of stability for the solutions with $\lambda=2, 3, 7/2, 4$, respectively. The dashed line 3 is $F = P/8$.

The energy of the trivial solution is equal to 0. Any other equilibrium solution which corresponds to a given λ has a negative energy per molecule

$$U_\lambda = - \left[\frac{F}{2F(\lambda)} - \frac{P}{P(\lambda)} + \frac{1}{2} \right]^2. \quad (3.10)$$

One can check that the energy U_λ does not depend on P and F along any line of the set

$$F = \frac{P(\lambda)}{2} P - D, \quad D \geq F(\lambda). \quad (3.11)$$

The lines of the set are parallel to the tangent to parabola 1 at the point $[P(\lambda), F(\lambda)]$.

Note, that Eqs. (3.7)–(3.11) are accurate only for $\lambda=2, 4$, i.e., for solutions (2.6) and (2.8). For any other λ they give a qualitatively good approximation.

Now one can choose any path in the phase space which crosses parabola 1 at the point $[P(\lambda), F(\lambda)]$ and compare the energy of the N -periodic IC structure with the energy of the N^* -periodic low-symmetry structure which is formed when the representative point moves away from the parabola. For simplicity let us consider the path $F=F(\lambda) = \text{const}$. The remainder between the energies is

$$\sqrt{|U_\lambda|} - \sqrt{|U_{\lambda^*}|} = P \left(\frac{1}{P(\lambda^*)} - \frac{1}{P(\lambda)} \right) - \frac{F(\lambda)}{2F(\lambda^*)} + \frac{1}{2}. \quad (3.12)$$

The condition $\sqrt{|U_\lambda|} - \sqrt{|U_{\lambda^*}|} = 0$ gives the critical value of P :

$$P_{\text{cr}} = 2 \frac{F(\lambda) - F(\lambda^*)}{P(\lambda) - P(\lambda^*)} \frac{P(\lambda)}{P(\lambda^*)}. \quad (3.13)$$

While $P \leq P_i = P(\lambda)$, the crystal has the high-symmetry phase (trivial solution). At $P = P_i$ the phase transition from the high-symmetry to IC phase takes place and the sinusoidal modulation is formed. The contribution of the higher harmonics increases as P moves from P_i to P_{cr} and for $P > P_{\text{cr}}$ the modulation takes the form which may be considered as a set of domains of the low-symmetry N^* -periodic commensurate phase which are separated by the discommensurations (domain walls).

In the following sections, the properties of the domain walls will be studied.

IV. TYPES OF DOMAIN WALLS

Let us describe the features of the set of domain walls in the structure with period $\lambda^* = N^*/M^*$ which appears as a result of the motion of the representative point along the path $F = \text{const}$ away from the point (P_{cr}, F) . The set of all the hinges of a chain is conveniently divided into N^* subsets. The subset with number i , where i may take one of the values $0, \dots, N^*-1$, contains the hinges with numbers $N^*n + i$, where n is any integer. Let us define on the i th subset the function v_i which takes the values equal to the displacements of the hinges of the subset. Since $N^* \ll N$, the oscillation of the functions v_i is much slower than that of the displacements y_n . In the immediate vicinity of parabola 1, the functions v_i are, in very good approximation, sinusoidal with the wavelength $\Lambda = N^*/\rho$. The function v_i is obtained by shifting v_{i+1} by Λ/N^* . The functions v_i tend to become the step functions as the distance from the critical point increases. The steps are formed at the places where at least one of the functions v_i changes the sign. It leads to the formation of KN^* steps within the wavelength Λ , where $K=1$ or 2 for an even or an odd number N^* , respectively. Clearly KN^* is an even number. All the KN^* walls within a wavelength Λ are different even though they have the same energy. In each wall within a period Λ the functions v_i with different numbers have the steps of specified height and sign. This difference is important as far as the possibility of the annihilation of domain walls is concerned. The wall with number j , where $j=1, \dots, KN^*/2$, can annihilate in principle only with the wall $j + KN^*/2$.

Except for the structure with $\lambda^*=2$, it is important whether $\lambda^* < \lambda$ or $\lambda^* > \lambda$. In the first case the domain wall is formed by adding one molecule into the ideal λ^* -periodic structure, but in the second case by the removal of a molecule. In what follows these domain walls will be called compressed and extended walls, respectively. The two types of walls in general differ energetically. Only in the two-periodic structure are the extended and compressed walls indistinguishable.

All of the preceding are illustrated in Figs. 4(a) and 4(b)

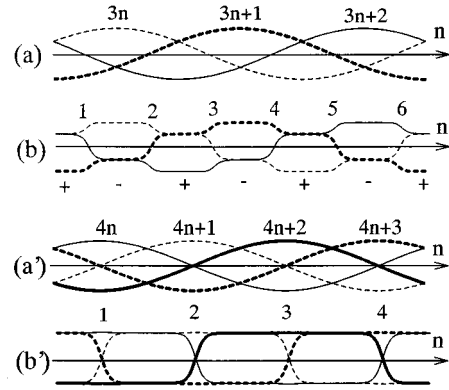


FIG. 4. Change of regime from a sinusoidal modulation to an array of domains in λ^* -periodic commensurate structure, (a), (b) for $\lambda^*=3$ and (a'), (b') for $\lambda^*=4$. The lines of different type correspond to the functions v_i . In the vicinity of parabola 1 [(a), (a')] the modulations are sinusoidal with the wavelength Λ . Rather far from the parabola in (b) we have six different domain walls within a period and in (b') there are four walls. The microscopic structure of the domain walls one can find in Fig. 3.

for the structure with $\lambda^*=3$ and Figs. 4(a') and 4(b) for $\lambda^*=4$. In Figs. 4(a) and 4(a'), the functions v_i in the vicinity of parabola 1, where they are sinusoidal with the wavelength Λ , are shown. In Figs. 4(b) and 4(b'), the functions v_i are shown at the moment when the representative point is rather far from parabola 1. For $\lambda^*=3$ we have $N^*=3$, $K=2$, and the number of domain walls within a period Λ is equal to 6. If $\lambda^*=4$ then $N^*=4$, $K=1$ and the number of domain walls within the period Λ is equal to 4. It is clear from Fig. 4(b') that domain wall 1 can annihilate, in principle, only with domain wall 3.

Summing up, the set of domain walls in an IC phase is the regular arranged system of walls of KN^* different types. One type of wall can annihilate, in principle, only with the wall of other specific type. If $\lambda^* < \lambda$, all the walls are the compressed ones, in the opposite case they are the extended ones.

V. PROPERTIES OF DOMAIN WALLS

A. Analytical solutions

Among the possible periodic structures the two- and four-periodic structures are fully considered. Let us obtain the approximate solution to Eq. (2.4) in the form of a moving domain wall in the periodic structures.

In the case $\lambda^*=2$, we consider two functions $v_i(n)$ instead of $y(n)$, one of which is defined on the hinges with the even numbers and the other on that with the odd numbers, moreover, $v_0 = -v_1 = v$. Equation (2.4) becomes

$$\frac{d^2 v_n}{d\tau^2} + F(v_{n-2} + 4v_{n-1} + 6v_n + 4v_{n+1} + v_{n+2}) - P(v_{n-1} + 2v_n + v_{n+1}) + v_n + v_n^3 = 0. \quad (5.1)$$

In the long-wave approximation, one obtains from Eq. (5.1)

$$V_{\tau\tau} + h_0^2(8F - P)V_{xx} + (16F - 4P + 1)V + V^3 = 0, \quad (5.2)$$

where $V(x, \tau)$ is the unknown slowly varying continuous function and $h_0 = h\sqrt{|r/s|}$. The numerical results of the present paper were obtained at $h_0 = 1$. Substituting $V(x, \tau) = V(x - c\tau)$ into Eq. (5.2) gives

$$V_{\xi\xi} + ABV - BV^3 = 0, \quad (5.3)$$

where $\xi = x - c\tau$, $A = 4P - 16F - 1$, $B = [h_0^2(P - 8F) - c^2]^{-1}$. The general solution to Eq. (5.3) is

$$\xi + \xi_0 = \int \left(E - ABV^2 + \frac{B}{2} V^4 \right)^{-1/2} dV, \quad (5.4)$$

where E, ξ_0 are the arbitrary constants. If $E = (A^2B)/2$ one obtains the solution in the form of a solitary wave:

$$V = \pm \sqrt{A} \tanh \left(\sqrt{\frac{AB}{2}} (\xi + \xi_0) \right). \quad (5.5)$$

With this result one can write the solution to Eq. (2.4) in the form of a moving domain wall in the two-periodic structure:

$$y_n = \pm (-1)^n \sqrt{A} \tanh \left(\sqrt{\frac{AB}{2}} [(n + n_0)h_0 - c\tau] \right). \quad (5.6)$$

There are two types of walls, + and -. For $|n| \rightarrow \infty$ Eq. (5.6) gives the solution (2.6). The solution exists if $A > 0$ and $AB > 0$. The first condition is condition (3.7) for the existence of the two-periodic solution. From the second condition it is clear that solution (5.6) exists not in the whole region where the two-periodic structure exists, but only in the region $F < P/8$. The solution of the considered type in the region $F > P/8$ should be found from Eq. (5.4). The width of the wall $\sqrt{2/(AB)}$ increases as the magnitude of AB tends to 0 and decreases as the velocity of the wall c is increased. The limiting value of the velocity is equal to $h_0^2\sqrt{P - 8F}$.

In the case $\lambda^* = 4$, we introduce four functions v_i defined on the hinges with the numbers $4n, 4n + 1, 4n + 2, 4n + 3$, respectively. From the numerical results shown in Fig. 4(b') one can see that for any type of walls they have the following symmetry: $v_0 = -v_2 = v$, $v_1 = -v_3 = w$. The equations for motion of the two neighboring hinges are

$$\begin{aligned} \frac{d^2 v_n}{d\tau^2} + F(-v_{n-2} + 4w_{n-1} + 6v_n - 4w_{n+1} - v_{n+2}) \\ - P(w_{n-1} + 2v_n - w_{n+1}) + v_n + v_n^3 = 0, \\ \frac{d^2 w_n}{d\tau^2} + F(-w_{n-2} - 4v_{n-1} + 6w_n + 4v_{n+1} - w_{n+2}) \\ - P(-v_{n-1} + 2w_n + v_{n+1}) + w_n + w_n^3 = 0. \end{aligned} \quad (5.7)$$

In the long-wave approximation after the substitution $V(x, \tau) = V(x - c\tau)$, $W(x, \tau) = W(x - c\tau)$, from Eqs. (5.7) one obtains

$$\begin{aligned} (c^2 - 4h_0^2F)V_{\xi\xi} + 2h_0(P - 4F)W_{\xi} \\ + (4F - 2P + 1)V + V^3 = 0, \end{aligned}$$

$$\begin{aligned} (c^2 - 4h_0^2F)W_{\xi\xi} - 2h_0(P - 4F)V_{\xi} \\ + (4F - 2P + 1)W + W^3 = 0, \end{aligned} \quad (5.8)$$

where $\xi = x - c\tau$. Note, that on the line $F = P/4$, the equations of systems (5.7) and (5.8) become independent. Under this condition the crystal splits into two embedded sublattices, in each of which the waves of the considered symmetry move without interaction.

Suppose that a domain wall is formed by an intersection of the functions $W(\xi)$ and $-W(\xi)$. Then the function $V(\xi)$ is almost constant \sqrt{A} and the terms with $V_{\xi\xi}, V_{\xi}$ may be omitted in Eqs. (5.8). The second equation takes the form (5.3) with the coefficients $A = 2P - 4F - 1$, $B = 1/(4h_0^2F - c^2)$ and its solitonlike solution is given by Eq. (5.5). Then the function $V(\xi)$ can be found from the first equation. It is convenient to simplify it by setting $V(\xi) = \sqrt{A} + \epsilon(\xi)$ and to linearize with respect to $\epsilon(\xi)$, in view of the smallness of the function $\epsilon(\xi)$. As a result one obtains

$$V(\xi) = \sqrt{A} - \frac{h_0}{A} (P - 4F)W_{\xi}. \quad (5.9)$$

Now the solution may be made more precisely. Substitution of Eq. (5.9) into the second equation of Eq. (5.8) gives a more exact equation for $W(\xi)$ in which only the coefficient B will be changed. The solution to Eq. (2.4) in the form of moving domain wall in the four-periodic structure may be written as

$$\begin{aligned} y_{4n} = \pm \sqrt{A} - \sqrt{\frac{B}{2}} h_0(P - 4F) \cosh^{-2} \left(\sqrt{\frac{AB}{2}} n' \right), \\ y_{4n+1} = \sqrt{A} \tanh \left(\sqrt{\frac{AB}{2}} n' \right), \\ y_{4n+2} = -y_{4n}, \\ y_{4n+3} = -y_{4n+1}, \end{aligned} \quad (5.10)$$

where $n' = h_0(n + n_0) - c\tau$, $A = 2P - 4F - 1$, $B = 1/(4h_0^2F - c^2)$ or more precisely $B = [4h_0^2F - (2h_0^2/A)(P - 4F)^2 - c^2]^{-1}$. There exist eight different domain walls. To describe the four compressed walls it is necessary to choose sign + in the first equation of Eqs. (5.10) and to shift the indices by unity sequentially. Four extended walls correspond to sign -. The solution exists if $A > 0$ and $AB > 0$, i.e., in the whole region where the four-periodic structure exists [see Eq. (3.7) for $\lambda = 4$]. For $|n| \rightarrow \infty$, Eqs. (5.10) give solution (2.8). On the line $F = P/4$ the motion of the domain wall in the sublattice with odd hinges does not influence the motion of the even hinges and they may be at rest.

B. Static properties of domain walls

In Fig. 5(a) the energy variation of the domain wall which is at rest ($c = 0$) in the two-periodic structure along the line (3.11) with $\lambda = 2$, $D = F(2) + 10^{-4}$ is plotted as a function of F . In Fig. 5(b), similar results are plotted for the extended wall (solid line) and the compressed wall (dashed line) in the four-periodic structure along the line (3.11) with $\lambda = 4$, $D = F(4) + 2 \times 10^{-3}$. Along the considered lines the energy of the corresponding structures does not change. Equations

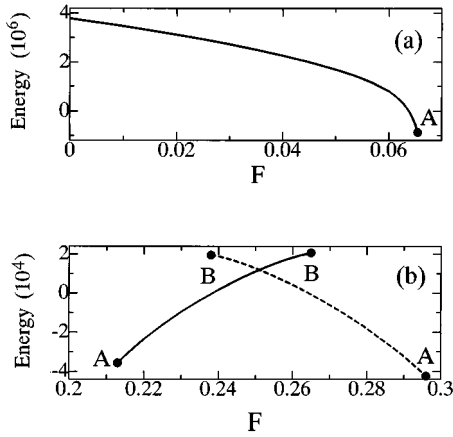


FIG. 5. The energy variation of the domain walls at $c=0$ as a function of F . In (a) the wall is in the two-periodic structure and the representative point moves along the line (3.11) with $\lambda=2$, $D=F(2)+10^{-4}$. In (b) the extended wall (solid line) and the compressed wall (dashed line) are in the four-periodic structure. The representative point moves along the line (3.11) with $\lambda=4$, $D=F(4)+2\times 10^{-3}$. At points A and B the walls become unstable.

(5.6) and (5.10) were used in the numerical calculations as the initial conditions. They give a good approximation in the region far from the boundary of their stability or existence. For two-periodic structure, the solution in region $F > P/8$ was found by slowly changing the parameters P, F along the considered line from the region where the solution is known. To avoid the oscillations which appeared in the region where the initial conditions were not exact, the dissipative term was added to Eq. (2.4).

We emphasize that the stable domain walls with a negative energy exist at some domains of parameter F . This is a consequence of the fact that inside these domains the ideal two- or four-periodic structures are metastable.

In Fig. 6(a), the change of the displacements of hinges near the domain wall in the two-periodic structure along the considered line (3.11) is shown for different parameters F . In

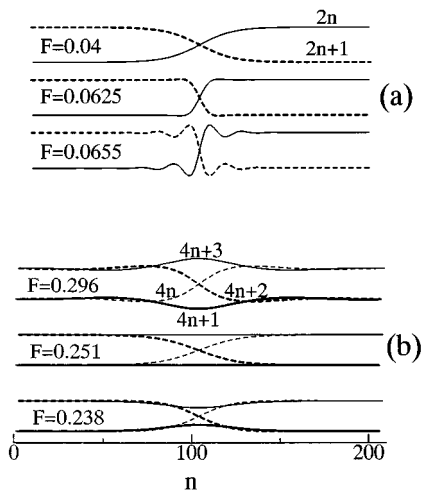


FIG. 6. The displacements of hinges near the domain wall at different F for (a) a domain wall in the two-periodic structure, $P=4F+1/4+10^{-4}$ and (b) a compressive domain wall in the four-periodic structure, $P=2F+0.5+2\times 10^{-3}$.

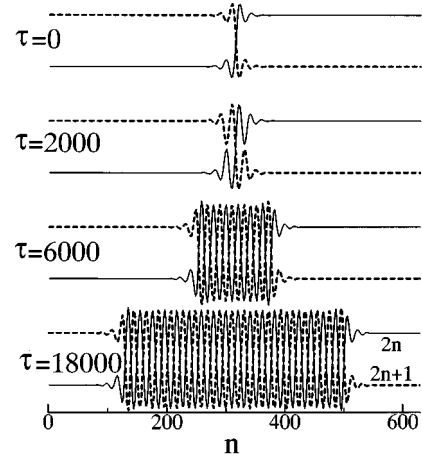


FIG. 7. The breakup of the unstable domain wall in the two-periodic structure into two autosolitons moving with a constant velocity in the opposite directions. $F=0.066$, $P=4F+1/4+10^{-4}$.

Fig. 6(b), the same results for a compressive domain wall in the four-periodic structure are presented.

C. Creation and annihilation of domain walls

The curves in Figs. 5(a) and 5(b) terminate at the points where the domain walls become unstable. In the points marked by the letter A, the domain wall breaks up into two autosolitons moving in opposite directions. The autosoliton transforms the ideal metastable two- or four-periodic structure into one of the structures with smaller energy. The energy given out provides the motion of the autosoliton with a constant velocity, even though there is the dissipation in the system. The domain wall fulfills the role of a nucleus of the new low-energy phase and that is why it can have negative energy. Formation and motion of the autosolitons in the two-periodic structure is presented in Fig. 7. This process has many features of the martensite transformation. It also may be initialized by a collision of two stable walls with negative energy.

In the points marked by the letter B in Fig. 5(b) the extended (compressed) domain wall with rather high positive energy breaks up into three compressed (extended) domain walls with energy about zero. One wall is at rest and two others move in opposite directions. This process is shown in Fig. 8.

Let us discuss the features of the collision of the domain walls. Equation (2.4) will be considered now without the dissipative term.

For the two-periodic structure in the region $F < P/8$, rather wide walls move along the crystal without the loss of energy but during the collision they necessarily lose a part of their kinetic energy and emit phonons. As a consequence of this feature, if the velocity of collision is less than a limiting value then the fusion of the walls takes place and their total energy is slowly dissipated along the chain. This process is shown in Fig. 9.

There is another channel of domain-wall annihilation when they can collide with a velocity higher than the fusion limiting value, but in this case no less than three walls must be involved in the collision. In Fig. 10, one can see the

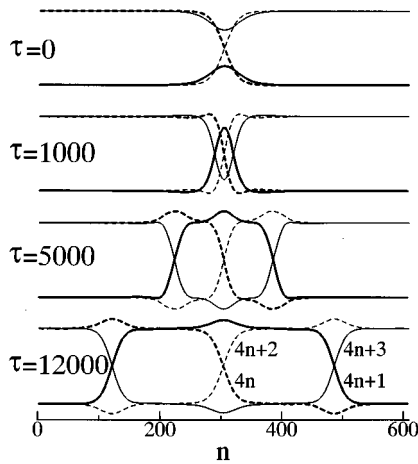


FIG. 8. The breakup of the unstable compressed domain wall in the four-periodic structure into three extended domain walls, one of which is at rest; two others move in opposite directions. The moving walls slow down due to the presence of the dissipation. $F=0.237$, $P=2F+0.5+2 \times 10^{-3}$.

collision of four walls with the annihilation of two of them and in Fig. 11 the same with the annihilation of all four walls. For this type of annihilation, the mutual arrangement of the walls at $\tau=0$ is not arbitrary. The changing of the relative positions of the walls may destroy the annihilation process.

Figures 9–11 are plotted for the coordinates of the representative point $F=0.04$, $P=4F+1/4+10^{-4}$ which is inside the region $F < P/8$. In this case the domain walls are attracted to one another if they are not too far from each other.

To study the collision between walls in the region $F > P/8$ we first obtained the walls with velocity $c=0$ by using the dissipative term and, second, we canceled the dissipative term and then two walls of opposite sign were accelerated toward each other by adding the term $(-1)^n \delta$ on the right-hand side of Eq. (2.4). This term describes the influence of an external field. After the walls were accelerated to the necessary velocity, this term was canceled as well. The walls in the region $F > P/8$ constantly radiate the phonons during the motion and so their velocity constantly reduces. The collision also leads to the emission of the phonons. In the region $F > P/8$ the walls are repelled from each other. That is why the cores of two colliding walls may not pass through each other if the velocity of collision is less than a limiting value.

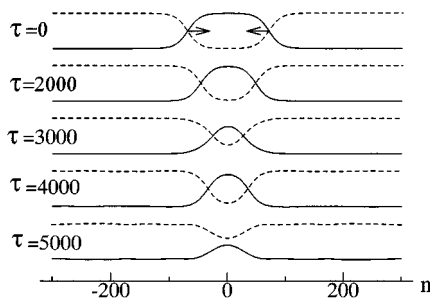


FIG. 9. Fusion of two domain walls in the two-periodic structure at $F=0.04$, $P=4F+1/4+10^{-4}$. The absolute value of the velocity of the walls $c=0.01$ is less than the fusion limiting value.

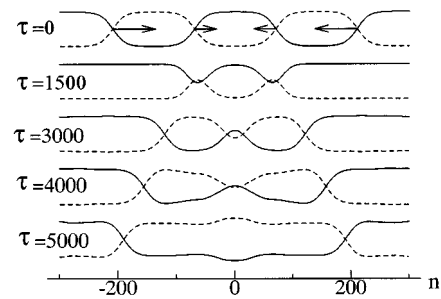


FIG. 10. The collision of four walls with the annihilation of two of them in the two-periodic structure at $F=0.04$, $P=4F+1/4+10^{-4}$. The absolute value of the velocity for slow walls is $c=0.022$ and for fast ones is $c=0.08$ which is larger than the fusion limiting value.

This is the difference from the case $F < P/8$. If the velocity of collision is very high the walls pass through each other. There is an intermediate range of the velocity when the kinetic energy of the walls is large enough for the cores to pass through each other, but not enough to go away from each other. In this range the annihilation of walls takes place.

In the four-periodic structure there are several types of domain walls and the number of collisions between different pairs of walls is rather high. Two general types of collisions are distinguished, the collision between the walls which can annihilate in principle and that between the walls which cannot annihilate. In the first case the behavior of the walls during the collision is very similar to the collision between walls in the two-periodic structure. The collision is accompanied by the loss of a part of the kinetic energy, there is the effect of fusion of slowly moving walls and there is the annihilation effect for many-walls collision. For the walls which cannot annihilate in principle, the loss of the energy and all the other manifestations of the collision are much smaller.

For the walls in the four-periodic structure, one new effect arises when the representative point is close to the line $F=P/4$. Mention has already been made that on this line Eqs. (5.7) and hence Eqs. (5.8) become independent. Near this line the extended and compressed walls have the same energy [see Fig. 5(b)]. In Fig. 12(a) one can see the result of a collision of two walls which can annihilate. The magni-

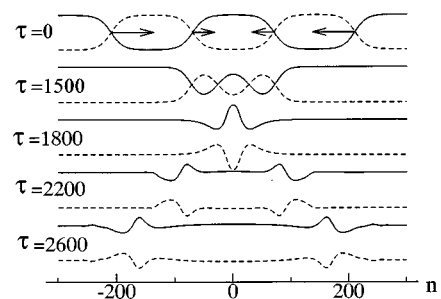


FIG. 11. The collision of four walls with the annihilation of all of them in the two-periodic structure at $F=0.04$, $P=4F+1/4+10^{-4}$. The absolute value of the velocity for slow walls is $c=0.026$ and for fast ones is $c=0.08$ which is larger than the fusion limiting value.

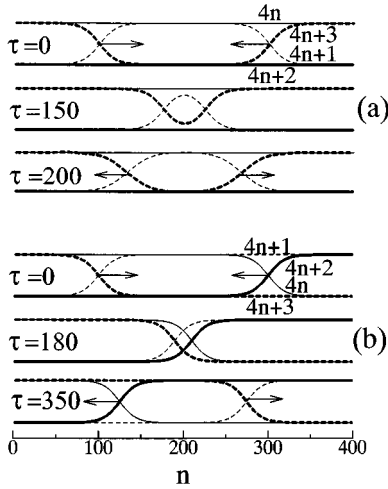


FIG. 12. The collision of two walls in the four-periodic structure at $F=0.251$, $P=2F+0.5+2 \times 10^{-3}$ which is near the line $F=P/4$. In (a) the case when walls can annihilate in principle is presented. Only the hinges with odd numbers are involved in the motion. The hinges with even numbers are at rest during the collision. In (b) the walls cannot annihilate in principle. They move in the different sublattices and do not interact with each other at all. They collide not only without loss of energy but even without the phase shift.

tudes of parameters are $F=0.251$, $P=2F+0.5+2 \times 10^{-3}$ which is near the line $F=P/4$. During the collision the phonons were emitted and the velocity of domain walls was decreased and their width increased. It is of interest that only the hinges with numbers $4n+1$ and $4n+3$ are involved in the motion. The hinges with even numbers are at rest not only during the motion of the walls along the chain but also during their collision. This effect manifests itself more clearly for the case of collision between the walls which cannot annihilate in principle. The results are depicted in Fig. 12(b) for the same magnitudes of parameters P, F . The walls move in different sublattices and they do not interact with each other at all. They collide not only without loss of energy but even without the phase shift.

In the region $F>P/4$ the compressed walls in the four-periodic structure repel each other, but in the region $F<P/4$ they attract each other. The opposite situation takes place for the extended walls.

D. Lock-in transition in the EHM model

Now we can describe the phase transformations along the path $F=\text{const}$. The case of phase transition from the high-symmetry phase to the commensurate four-periodic structure through the IC phase will be discussed.

As an example let us consider the phase transformations along the path $F=F(\lambda)$ for $\lambda=77/19$. In Fig. 13(a), the phase diagram in the vicinity of the point $[P(77/19), F(77/19)]=(1.02082, 0.26052)$ is schematically shown. The point $[P(\lambda^*), F(\lambda^*)]=[P(4), F(4)]$ has coordinates (1, 0.25). We kept the notations which were used in Fig. 2 for parabola $F=P^2/4$ (curve 1) and for the hyperbola (3.8) with $\lambda=4$ (curve 7). Curve a is the hyperbola (3.8) with $\lambda=77/19$ and line b is $F=P/4$. The dashed horizontal line is the considered path of the representative point which moves from left

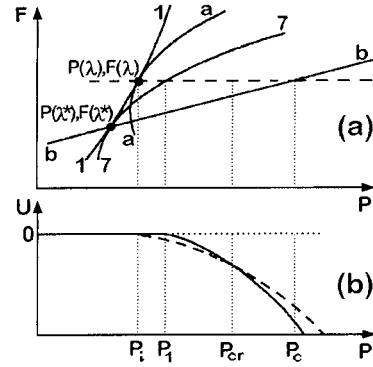


FIG. 13. Schematic representation of (a) the phase diagram in the vicinity of the point $[F(\lambda), P(\lambda)]=[F(77/19), P(77/19)]$ and (b) the P dependence of the energy along the path $F=F(77/19)$ for the ideal four-periodic solution (solid line) and for the 77-periodic solution depicted in Figs. 3(a')–3(c') (dashed line). Curve 1 in (a) is the parabola $F=P^2/4$; curves 7 and a are the hyperbolas (3.8) for $\lambda=4$, $77/19$, respectively; line b is $F=P/4$ and the dashed horizontal line is the path of the representative point which moves from left to right. The curves in (b) cross each other at a value P_{cr} . While $P \leq P_i = P(77/19)$, the crystal has the high-symmetry phase (trivial solution) with the energy $U=0$. The contribution of the higher harmonics increases as P moves from P_i to P_{cr} and for $P > P_{cr}$ there appear the domains of the low-symmetry four-periodic commensurate phase separated by the discommensurations. P_c corresponds to the lock-in transition. In the region $P > P_c$ there exists an ideal four-periodic structure.

to right. In Fig. 13(b), we schematically compare the energy of the ideal four-periodic solution (2.8) (solid line) with the energy of the 77-periodic solution depicted in Figs. 3(a)–3(c) (dashed line) along the path. These two curves are defined by Eq. (3.10) at $\lambda=4$ and $\lambda=77/19$, respectively.

While $P \leq P_i = P(77/19)$, the crystal has the high-symmetry phase (trivial solution) with the energy $U=0$. When the representative point crosses parabola 1, the phase transition from the high-symmetry to the IC phase takes place. In the vicinity of the parabola the modulation has a sinusoidal form. The solid line in Fig. 13(b) starts from the point with abscissa $P_i=1.02115$ which corresponds to the intersection between the path and the hyperbola 7 in Fig. 13(a). The curves depicted in Fig. 13(b) cross each other at the point $P_{cr}=1.0316$, defined by Eq. (3.13). The contribution of the higher harmonics increases as P changes from P_i to P_{cr} and for $P > P_{cr}$ in the crystal there are domains of the low-symmetry four-periodic commensurate phase separated by the compressed domain walls. In the region $F>P/4$ the compressed domain walls are mutually repulsive which makes them equally spaced. The walls start to attract each other when line b is crossed by the representative point ($F>P/4$). The abscissa of this point is denoted as P_c . One can find that $P_c=1.04208$. The equidistant arrangement of the mutually attractive walls becomes unstable and when the attraction becomes strong enough they start move and annihilate. The thermal fluctuations can play a role of perturbation of the positions of the walls and can help to overcome the Peierls barrier.⁷ The energy of the walls near the line $F=P/4$ is positive [see Fig. 5(b)]; that is why their annihilation

lation is the phase transition of the first-order (the lock-in transition). In the region $P > P_c$ there exists the ideal four-periodic structure.

It should be emphasized that the point P_c is not critical for four-periodic structure itself, but it is critical for the set of domain walls. Therefore in this model the lock-in transition can be regarded as the phase transition in the domain-wall subsystem.

VI. CONCLUSION

First, the phase diagram of the proposed one-dimensional crystal model was obtained in the P, F plane nearby the boundary of stability of the trivial solution. The motion of the representative point in the phase space along a path with constant F was studied. It was shown that the crossing of the boundary at the point $[P(\lambda), F(\lambda)]$, where $\lambda = N/M$ has a big denominator, leads to the formation of a structure with long period $N > 2M$ (IC structure). When the representative point moves away from the boundary of trivial solution stability, one of the solutions with a significantly smaller denominator M^* and with a wavelength $\lambda^* = N^*/M^*$ which is close to $\lambda = N/M$ is formed (low-symmetry N^* -periodic commensurate phase, $N^* \ll N$). As a result of the process a system of regularly arranged domain walls appears.

Second, the properties and the behavior of the domain walls in two- and four-periodic structures were studied by solving the equation of the motion numerically. It was shown that if $\lambda^* < \lambda$, the set of domain walls contains KN^* compressed walls of different types, where $K = 1$ or 2 if N^* is an

even or an odd number, respectively; otherwise it contains the same number of extended walls. A certain type of wall can annihilate with walls of only one different type. The channels of the annihilation of the walls were found. The mechanisms of the annihilation make it possible to understand the nature of the lock-in phase transition. It is the phase transition in the domain-wall subsystem.

In the metastable periodic structure coexisting with the IC structure, the domain wall with a negative energy can exist. At some magnitudes of parameters P and F such a wall becomes unstable and breaks up into two autosolitons moving in the opposite directions. The autosolitons transform the ideal periodic structure into one of the structures with a smaller energy. This phase transition is a kind of the martensite transition. The transition may be initialized also by the collision of two stable walls with a negative energy.

For the four-periodic structure the relationship between P and F at which the crystal splits into two independent, embedded sublattices was found. Under this condition, waves of specified symmetry of hinge displacements move in different sublattices without interaction. For example, two domain walls moving in different sublattices collide not only without loss of the energy but even without the phase shift.

ACKNOWLEDGMENTS

The authors would like to thank T. A. Aslanian for discussions and fruitful comments. The work was partly supported by the Ministry of Education, Science and Culture of Japan.

*Permanent address: General Physics Dept., Barnaul State Technical University, 46, Lenin st., 656099, Barnaul, Russia.

¹*Incommensurate Phases in Dielectrics*, edited by R. Blinc and A. P. Levanyuk (North-Holland, Amsterdam, 1986), Vol. 1 and Vol. 2.

²J. C. Toledano and P. Toledano, *Landau Theory of Phase Transitions* (World-Scientific, Singapore, 1987).

³H. Bestgen, *Solid State Commun.* **58**, 197 (1986).

⁴H. Sakata, K. Hamano, X. Pan, and H.-G. Unruh, *J. Phys. Soc. Jpn.* **59**, 1079 (1990).

⁵K. Hamano, J. Zhang, K. Abe, T. Mitsui, H. Sakata, and K. Ema, *J. Phys. Soc. Jpn.* **65**, 142 (1995).

⁶T. A. Aslanian and A. P. Levanyuk, *Solid State Commun.* **31**, 547 (1979).

⁷*Solitons*, edited by S. E. Trullinger, V. E. Zakharov, and V. L. Pokrovsky (North-Holland, Amsterdam, 1986).

⁸F. Axel and S. Aubry, *J. Phys. C* **14**, 5433 (1981).

⁹T. Janssen and J. A. Tjon, *Phys. Rev. B* **25**, 3767 (1982).

¹⁰Z. Y. Chen and M. B. Walker, *Phys. Rev. B* **43**, 5634 (1991).

¹¹K. Parlinski, *Phys. Rev. B* **48**, 3016 (1993).

¹²S. Aubry, *J. Chem. Phys.* **64**, 3392 (1976).

¹³K. Parlinski, *Ferroelectrics* **104**, 73 (1990).

¹⁴K. Parlinski and F. Dénoyer, *Phys. Rev. B* **41**, 11 428 (1990).

¹⁵K. Parlinski, Y. Watanabe, K. Ohno, and Y. Kawazoe, *Phys. Rev. B* **50**, 16 173 (1994).

¹⁶K. Abe, K. Kawasaki, K. Kowada, and T. Shigenari, *J. Phys. Soc. Jpn.* **60**, 404 (1991).

¹⁷G. Dolino, P. Bastie, B. Berge, M. Vallade, J. Bethke, L. P. Regnault, and C. M. E. Zeyen, *Europhys. Lett.* **3**, 601 (1987).

¹⁸K. Gesi, *Jpn. J. Appl. Phys.* **4**, 818 (1965).

¹⁹E. Rapoport, *J. Chem. Phys.* **45**, 2721 (1966).

²⁰S. V. Dmitriev, K. Abe, and T. Shigenari, *J. Phys. Soc. Jpn.* **65**, 3938 (1996).